Electronic Supplementary Material (ESI) for Catalysis Science & Technology.

(Supporting Information)

Comparative study of the mobility of Pd species in SSZ-13 and ZSM-5, and its implication for catalytic activity after hydro-thermal aging as Passive NO_x Adsorbers (PNAs) for cold-start applications

Jaeha Lee[1], YoungSeok Ryou[1], Sungha Hwang[1], Yongwoo Kim[1], Sung June Cho[2], Hyokyoung Lee[3], Chang Hwan Kim[3], Do Heui Kim[1]*

[1]School of Chemical and Biological Engineering, Institute of Chemical Processes, Seoul National University, Seoul, 151-744 Republic of Korea

[2]Clean Energy Technology Laboratory and Department of Applied Chemical Engineering, Chonnam National University, Gwangju 500-757, Republic of Korea

[3]Hyundai-Kia Motors R&D center, Hwaseong, 445-706 Rep. of Korea

Corresponding author: dohkim@snu.ac.kr

Additional data; Table S1-S3, Figure S1-S15

sample		Pd (wt%) [1]	Pd/Al [1]
Pd(2)/ZSM-5 (30)	as synthesized	1.9	0.24
	after HTA	2.0	0.25
Pd(2)/ZSM-5 (50)	as synthesized	1.9	0.41
	after HTA	2.1	0.43
Pd(2)/SSZ-13 (35)	as synthesized	2.1	0.21
	after HTA	2.1	0.24

Table S1. Pd loading and Pd to Al molar ratio of Pd/ZSM-5 (30 and 50) and Pd/SSZ-13 (35) catalysts.

[1.] Measured from ICP-AES

Sample	Pair	CN	Distance (R_{eff}) (Å)	σ^2 (Å^2)	ΔE (eV)	R-factor
Pd(1)/SSZ-13 (35) 750C	Pd-O	3.62±0.35	2.02±0.00	0.001±0.001	3.96±1.26	0.039
	Pd-O-Pd	-	-	-	-	-
Pd(1)/SSZ-13 (35) 750C HTA	Pd-O	3.79±0.39	2.02±0.00	0.001±0.001	3.09±1.38	0.049
	Pd-O-Pd	-	-	-	-	-
Pd(2)/SSZ-13 (35) 750C	Pd-O	3.70±0.50	2.02±0.00	0.001±0.001	6.02±1.48	0.059
	Pd-O-Pd	-	-	-	-	-
Pd(2)/SSZ-13 (35) 750C HTA	Pd-O	3.45±0.65	2.02±0.01	0.001±0.001	4.10±2.20	0.084
	Pd-O-Pd	1.28±1.24	3.03±0.05	0.002±0.004	4.10±2.20	0.084
Pd(2)/ZSM-5 (30) 750C	Pd-O	3.30±0.20	2.01±0.00	0.001±0.001	11.0±0.00	0.004
	Pd-O-Pd	-	-	-	-	-
Pd(2)/ZSM-5 (30) 750C HTA	Pd-O	3.55±0.65	2.02±0.01	0.001±0.001	4.50±2.20	0.085
	Pd-O-Pd	1.24±1.33	3.07±0.05	0.002±0.005	4.50±2.20	0.085
Pd(2)/ZSM-5 (50) 750C	Pd-O	3.55±0.74	2.02±0.02	0.001±0.001	3.94±2.29	0.087
	Pd-O-Pd	2.12±1.72	3.03±0.02	0.003±0.003	3.94±2.29	0.087
Pd(2)/ZSM-5 (50) 750C HTA	Pd-O	3.32±0.86	2.01±0.00	0.001±0.002	1.70±3.68	0.048
	Pd-O-Pd	2.63±2.98	3.03±0.04	0.023±0.017	1.70±3.68	0.048
Pd(2)/ZSM-5 (30) 750C 350V	Pd-O	1.50±0.59	2.02±0.02	0.004±0.004	0.49±0.64	0.019
	Pd-Pd	6.90±0.65	2.66±0.07	0.006±0.001	0.49±0.64	0.019
Pd(2)/SSZ-13 (35) 750C 350V	Pd-O	2.81±0.32	2.01±0.00	0.001±0.001	2.23±0.87	0.029
	Pd-Pd	2.94±0.52	2.67±0.08	0.006±0.001	2.23±0.87	0.029

Table S2. Summary of the curve-fitting of Pd K edge EXAFS data for Pd(2)/ZSM-5 (30 and 50) and Pd(1, 2)/SSZ-13 (35), after various thermal treatments.

Catalysts	Si to Al_2 molar ratio	NO_x storage ability (µmol/$g_{catal.}$)	
		before HTA	after HTA
Pd(2)/Modernite	20	24.1	4.3
Pd(2)/Beta	38	19.6	4.8

Table S3. The NO_x storage abilities of Pd(2)/Modernite and Pd/Beta catalysts, before and after the HTA treatment.

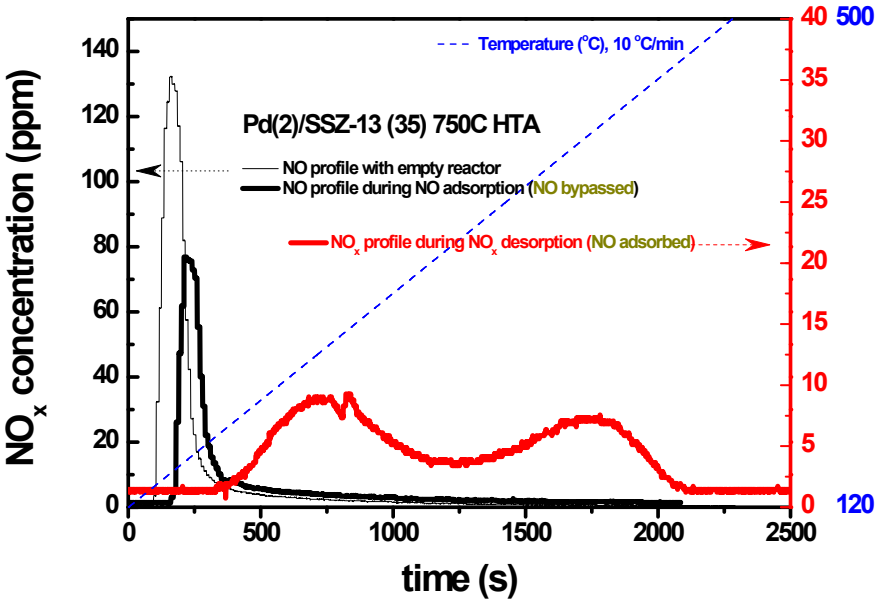

Pd(2)/SSZ-13 (35) 750C HTA

NO bypassed (µmol)	NO adsorbed (µmol)	Sum (µmol)	NO blank (µmol)
1.23	0.88	2.11	2.13

Figure S1. NO_x concentration measured during the NO_x adsorption/desorption test, and that measured with the empty reactor.

(a) **SSZ-13** (35)

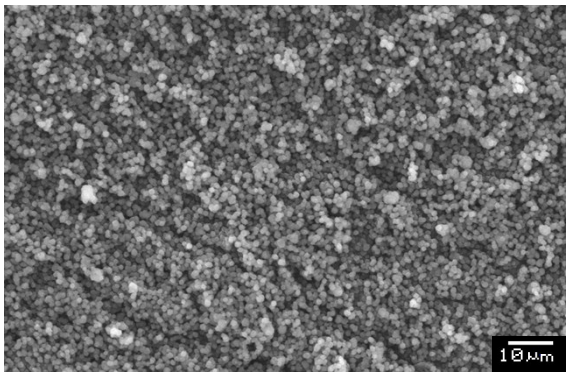

(b) **ZSM-5** (30)

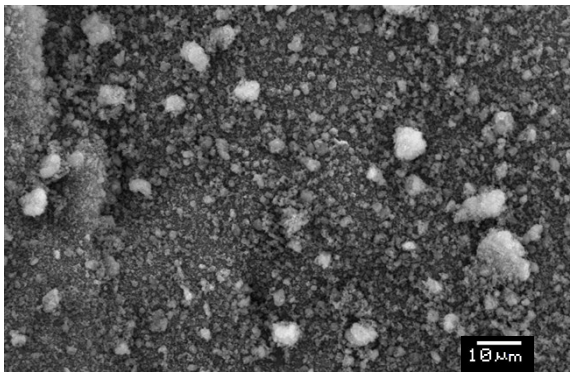

(c) **ZSM-5** (50)

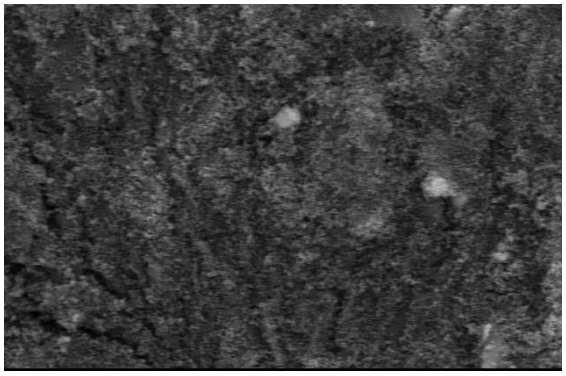

Figure S2. Representative SEM images of (a) SSZ-13 (35), (b) ZSM-5 (30), and (c) ZSM-5 (50).

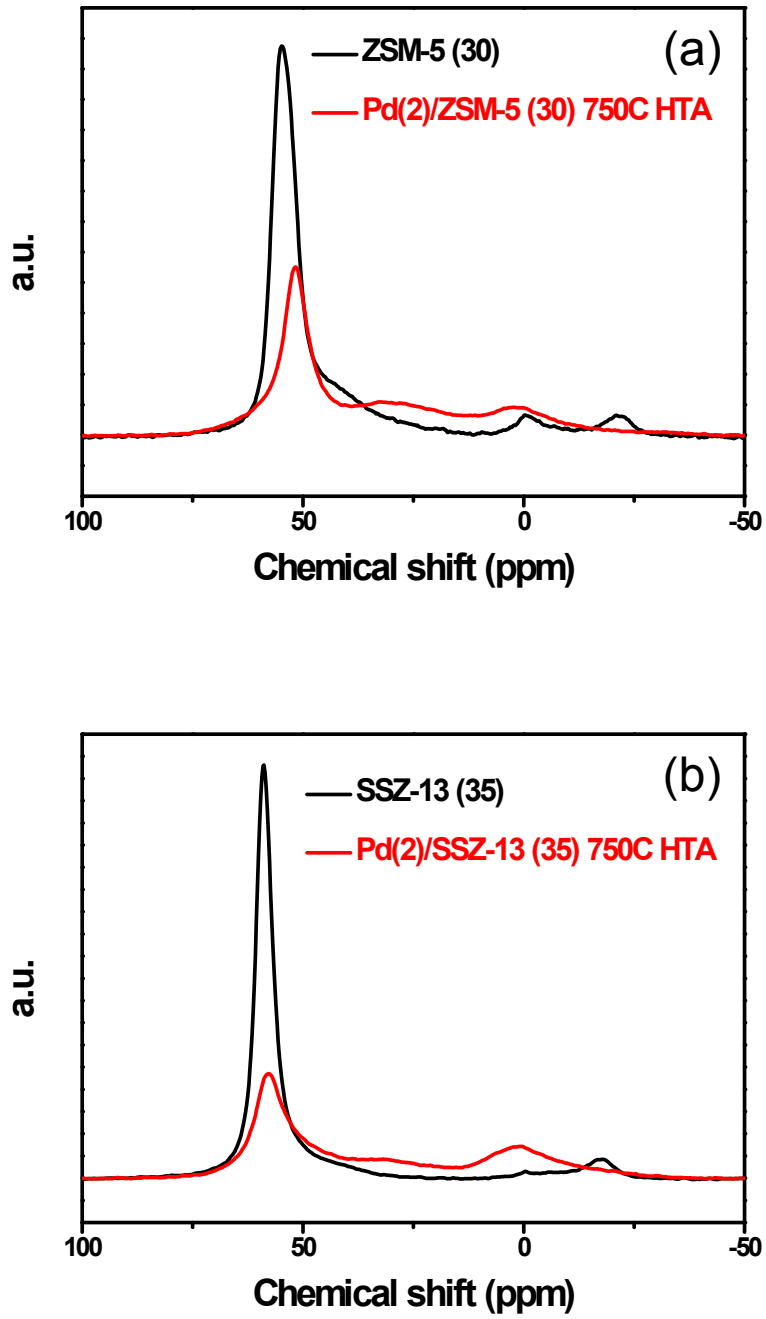

Figure S3. Al-NMR spectra of (a) ZSM-5 & Pd(2)/ZSM-5, and (b) SSZ-13 & Pd(2)/SSZ-13 catalysts. After the HTA treatment, the portion of frame-work Al was leached out, giving rise to the pentahedral and octahedral Al peaks at (22 and 0) ppm, respectively.

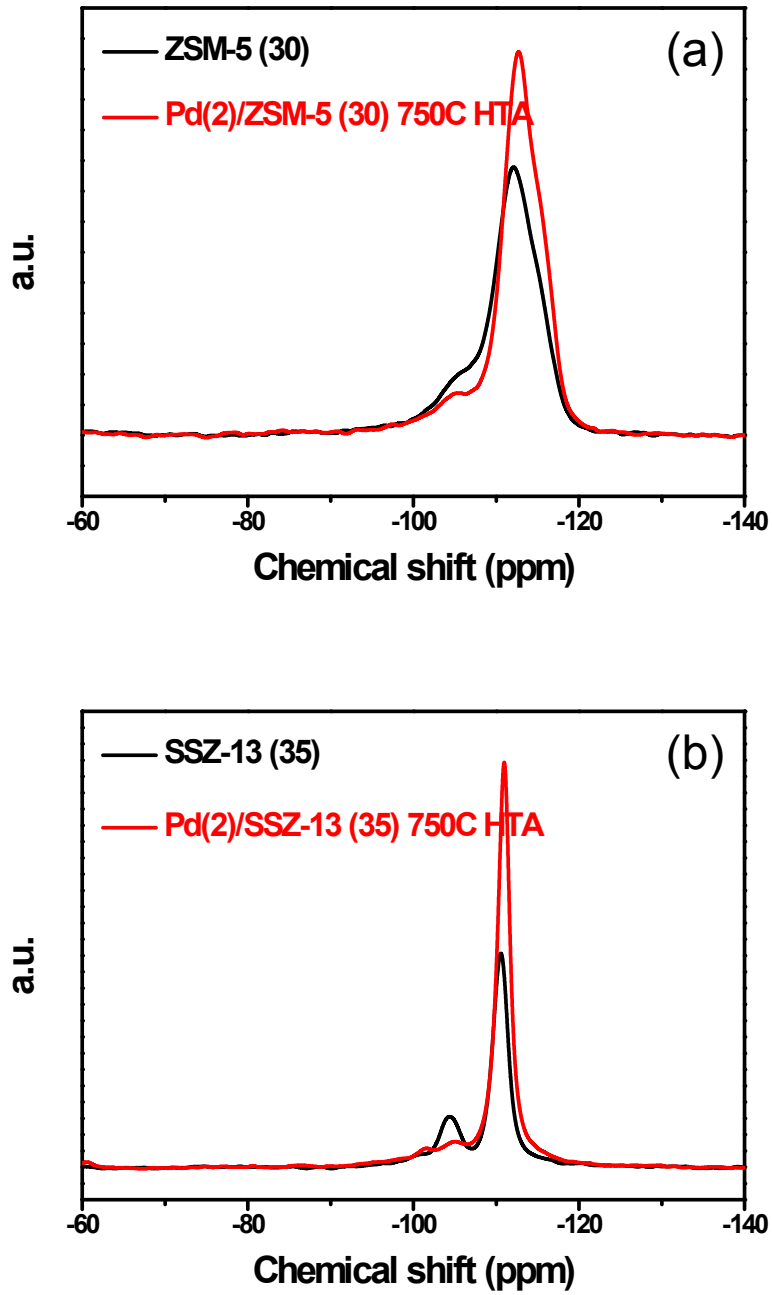

Figure S4. Si-NMR spectroscopy of (a) ZSM-5 & Pd(2)/ZSM-5, and (b) SSZ-13 & Pd(2)/SSZ-13 catalysts. After the HTA treatment, a part of the frame-work Al species was leached out, giving rise to the Si species that are less coordinated to Al species.

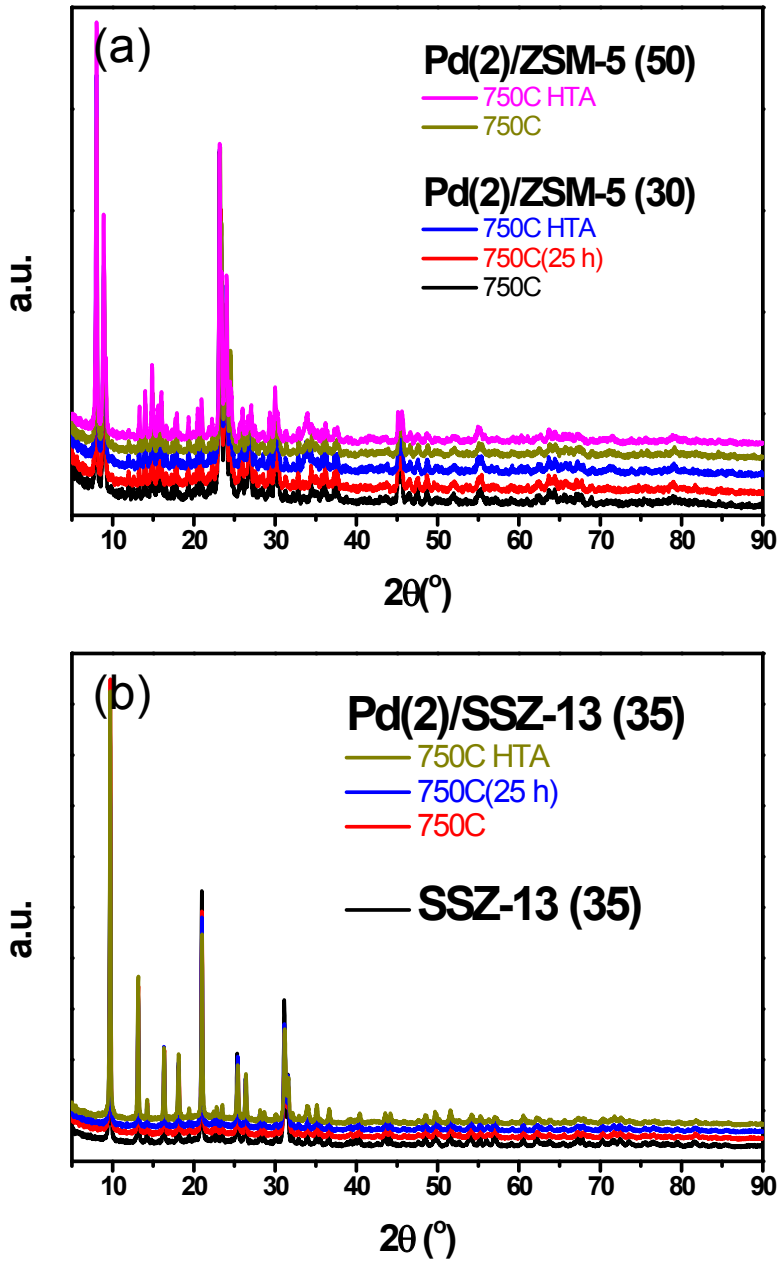

Figure S5. (a) XRD patterns of Pd(2)/ZSM-5 (30 and 50), and (b) XRD patterns of Pd(2)/SSZ-13 (35), after the oxidative process at 750 °C, or after the HTA treatment.

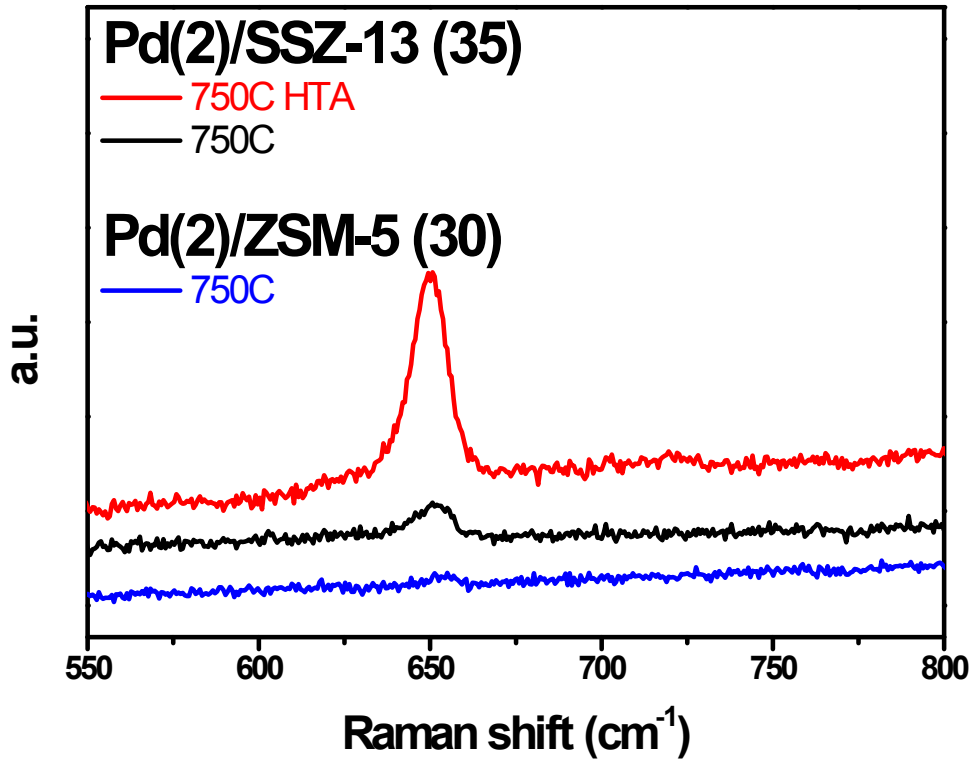

Figure S6. Raman spectra of Pd(2)/ZSM-5 (30) and Pd(2)/SSZ-13 (35). After the HTA treatment, the Raman intensity from the bulk PdO was greatly increased on Pd(2)/SSZ-13.

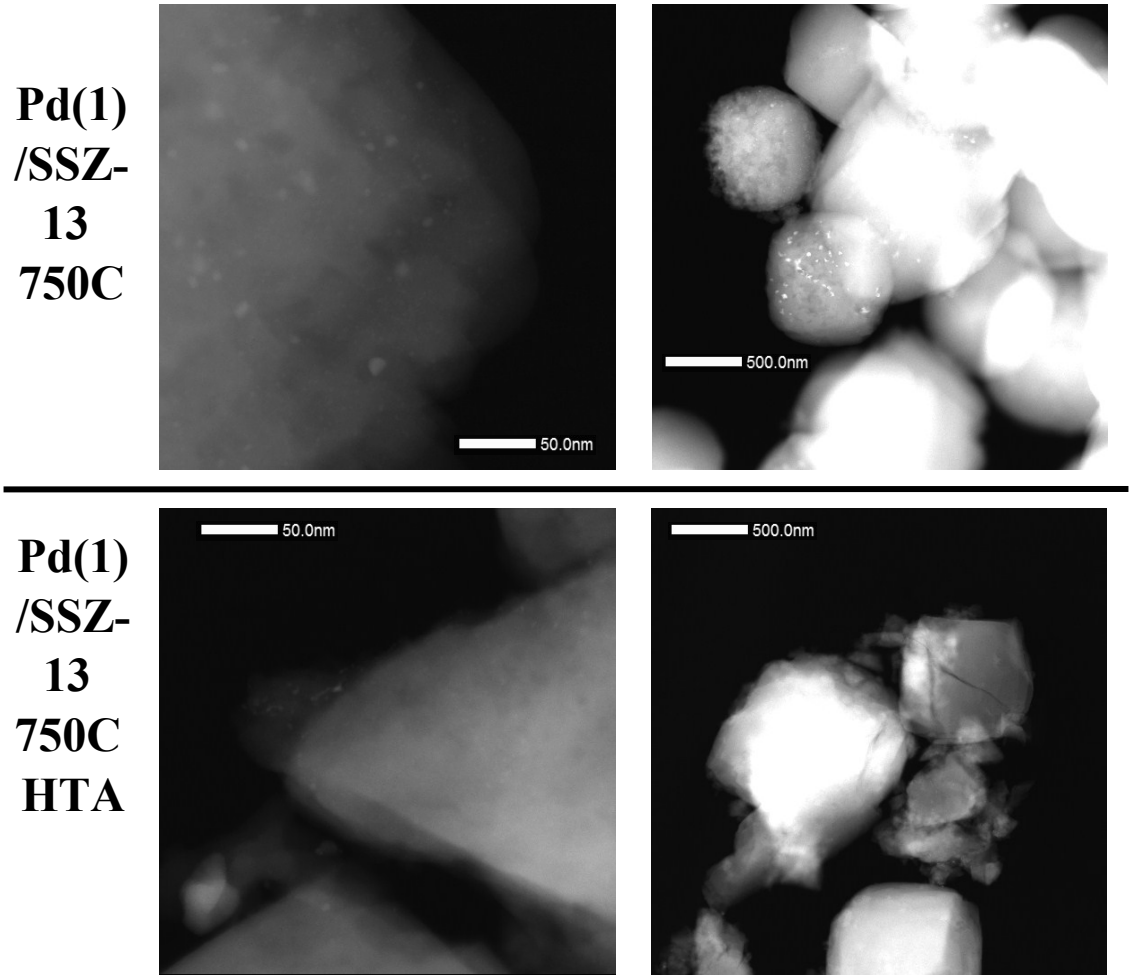

Figure S7. Representative HAADF-STEM images of Pd(1)/SSZ-13 (35) 750C (top) and Pd(1)/SSZ-13 (35) 750C HTA (bottom) catalysts.

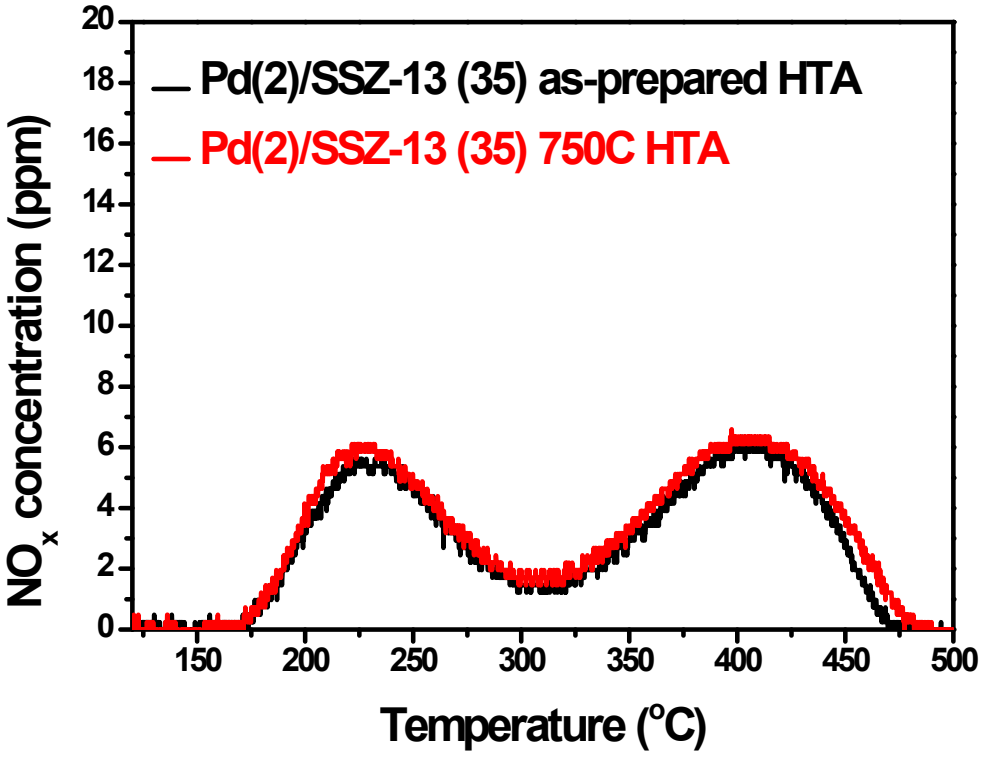

Figure S8. The NO_x desorption curves of the Pd(2)/SSZ-13 catalyst after the hydrothermal treatment. The identical curves were observed on the as-prepared catalyst and the 750C treated catalyst after the hydrothermal treatment.

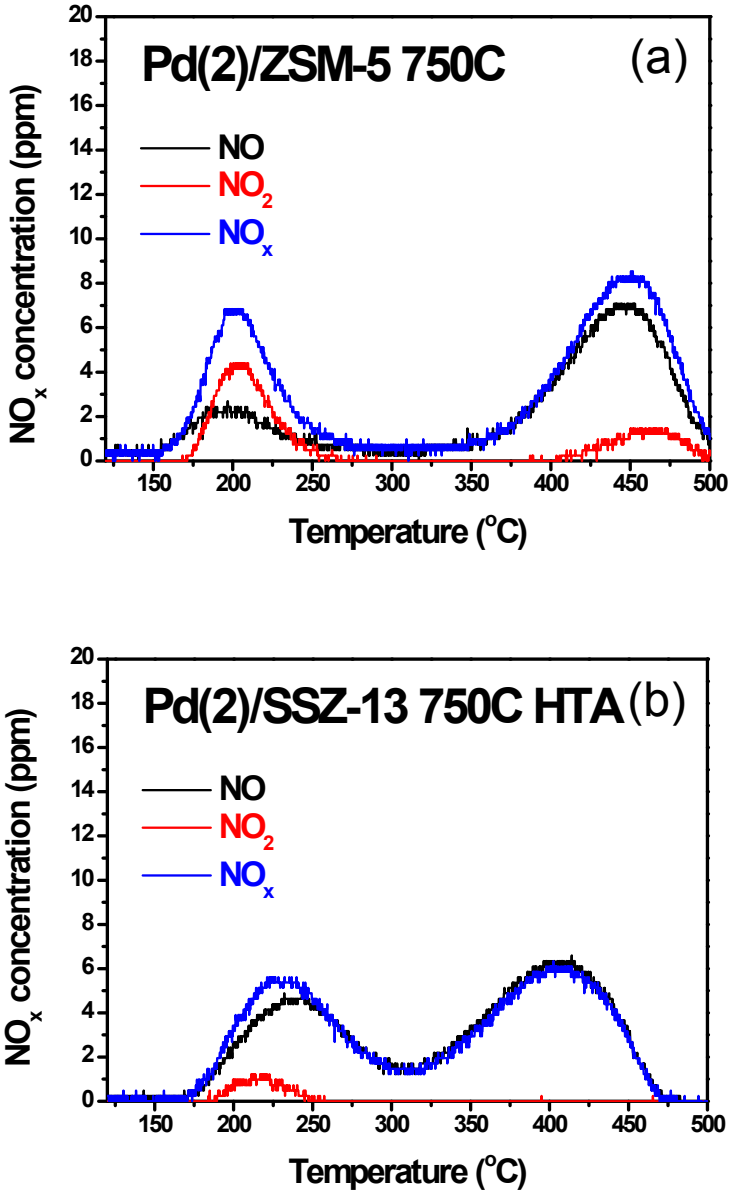

Figure S9. The NO, NO_2 and NO_x desorption curves of the (a) Pd(2)/ZSM-5 (30) 750C and (b) Pd(2)/SSZ-13 (35) 750C HTA catalysts.

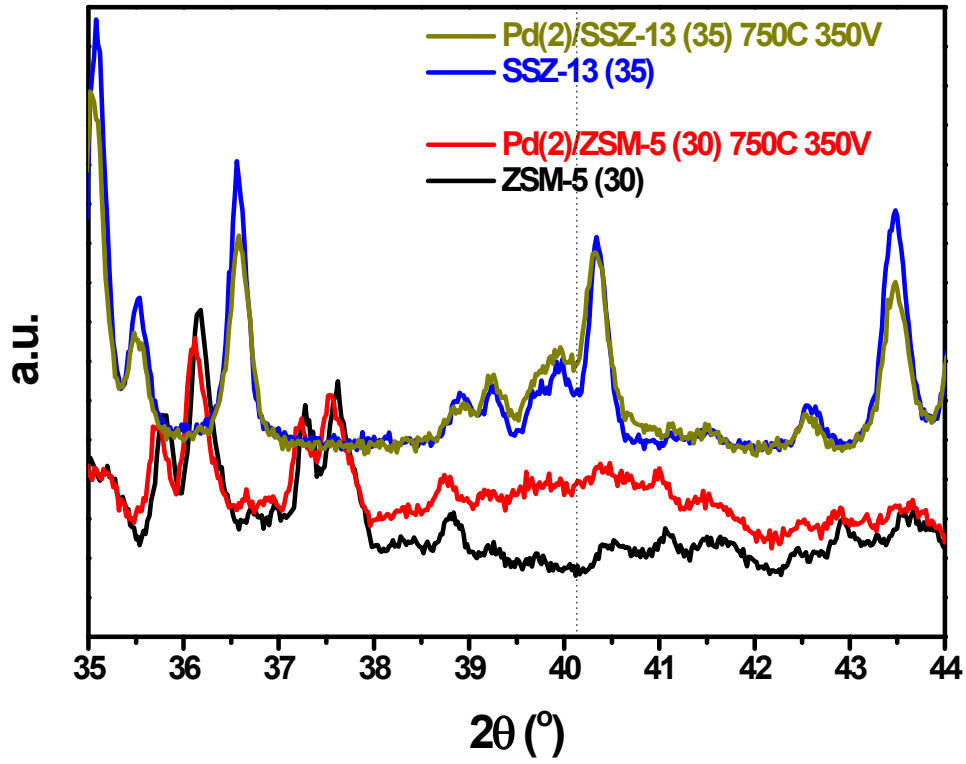

Figure S10. XRD pattern of ZSM-5 (30), Pd(2)/ZSM-5 (30) 750C 350V, SSZ-13 (35) and Pd(2)/SSZ-13 (35) 750C 350V catalysts. The 2θ region between (35 and 44)° was fine-scanned with the scan rate of 0.02 °/min.

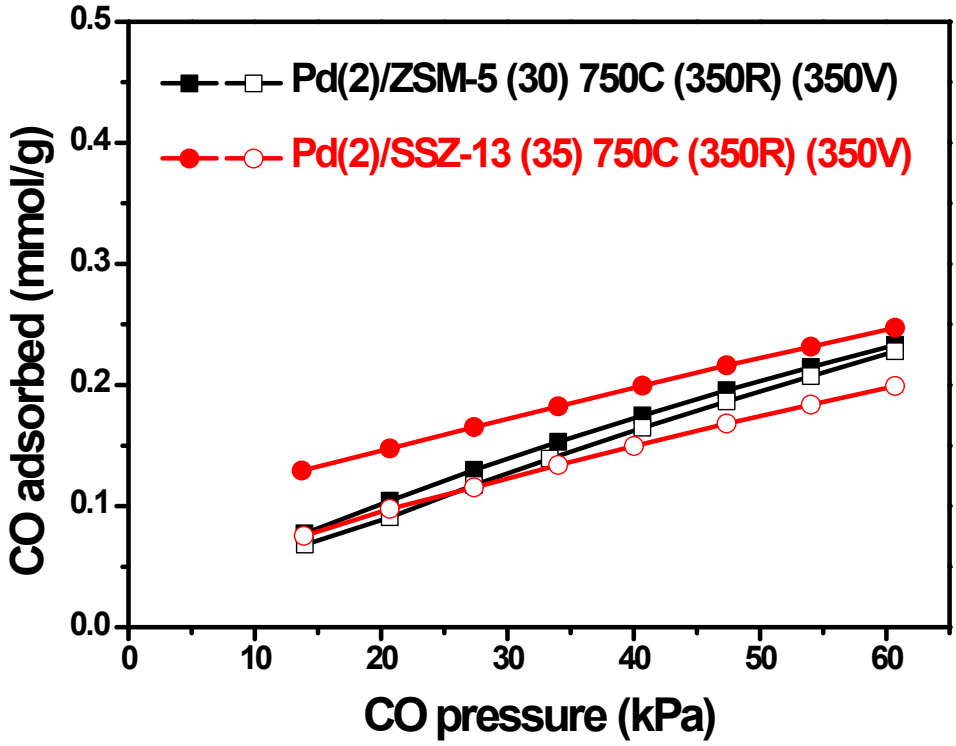

Figure S11. CO chemisorption curves of Pd(2)/ZSM-5 (30) 750C (350R) (350V) and Pd(2)/SSZ-13 (35) 750C (350R) (350V) catalysts. After obtaining the first isotherm (filled symbol), catalysts were evacuated at 35 °C for 4 h to obtain the second isotherm (empty symbol). The difference between two curves corresponds to the amount of chemisorbed CO.

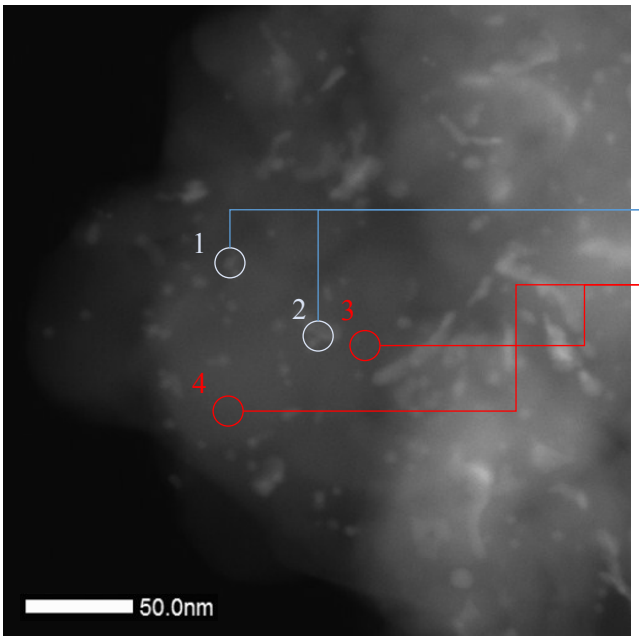

Both Pd and Al (1, 2)

Only Al (3, 4)

point	Pd (wt%)	Al (wt%)
1	95	5
2	81	19
3	0	100
4	0	100

Figure S12. EDX point analysis (Pd and Al) of the representative HAADF-STEM image of Pd(2)/ZSM-5 (30) 750C 350V.

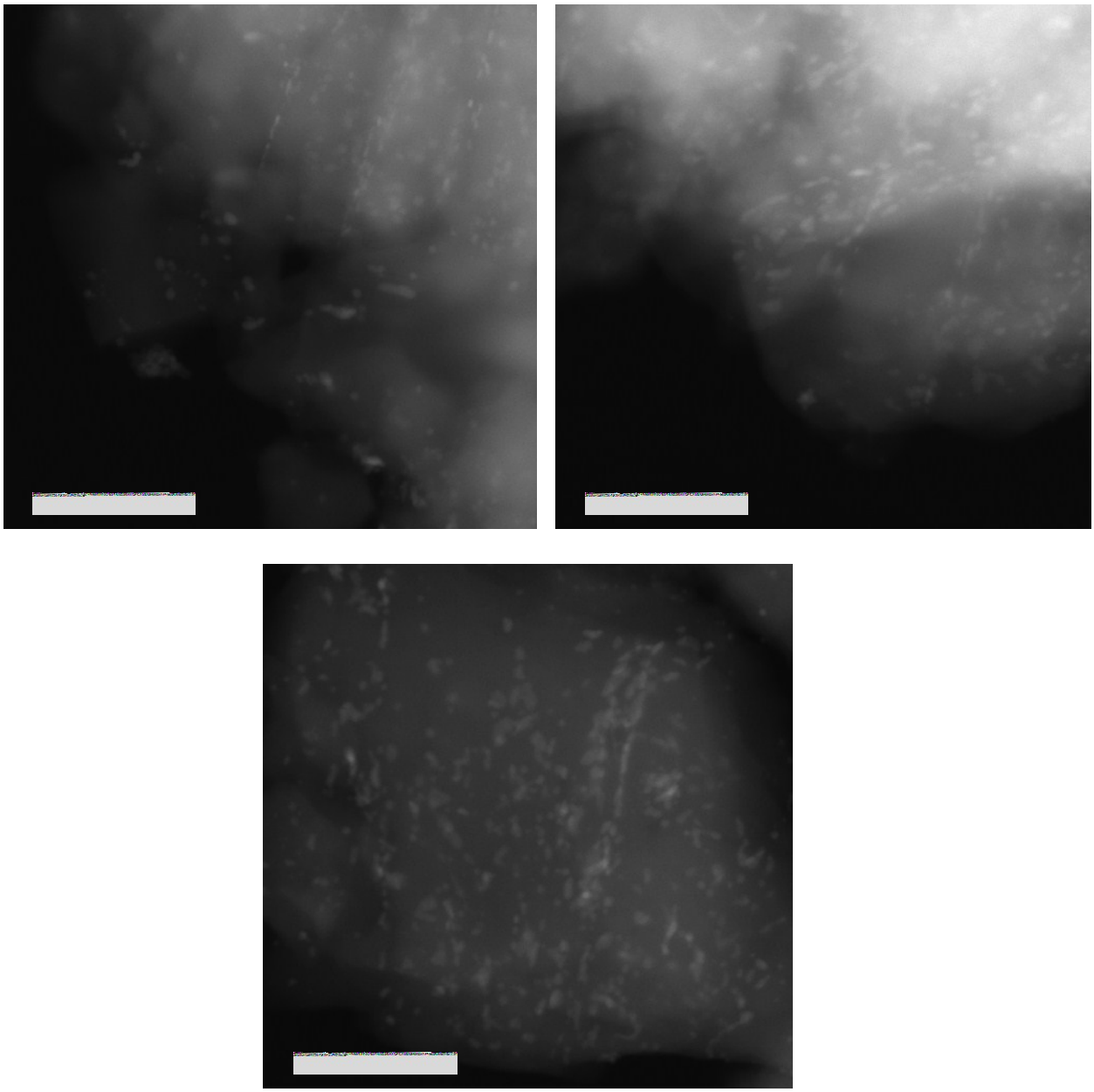

Figure S13. Representative HAADF-STEM images of Pd(2)/ZSM-5 (30) 750C 350V.

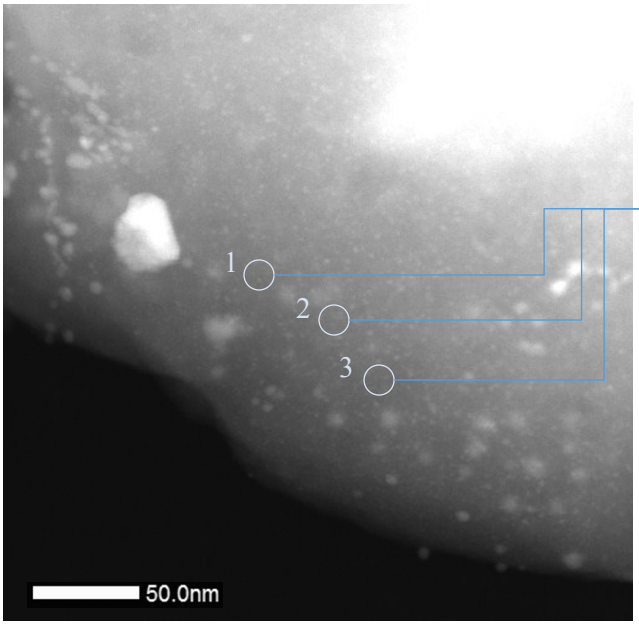

point	Pd (wt%)	Al (wt%)
1	65	35
2	69	31
3	46	54

Figure S14. EDX point analysis (Pd and Al) of the representative HAADF-STEM images of Pd(2)/SSZ-13 (35) 750C 350V.

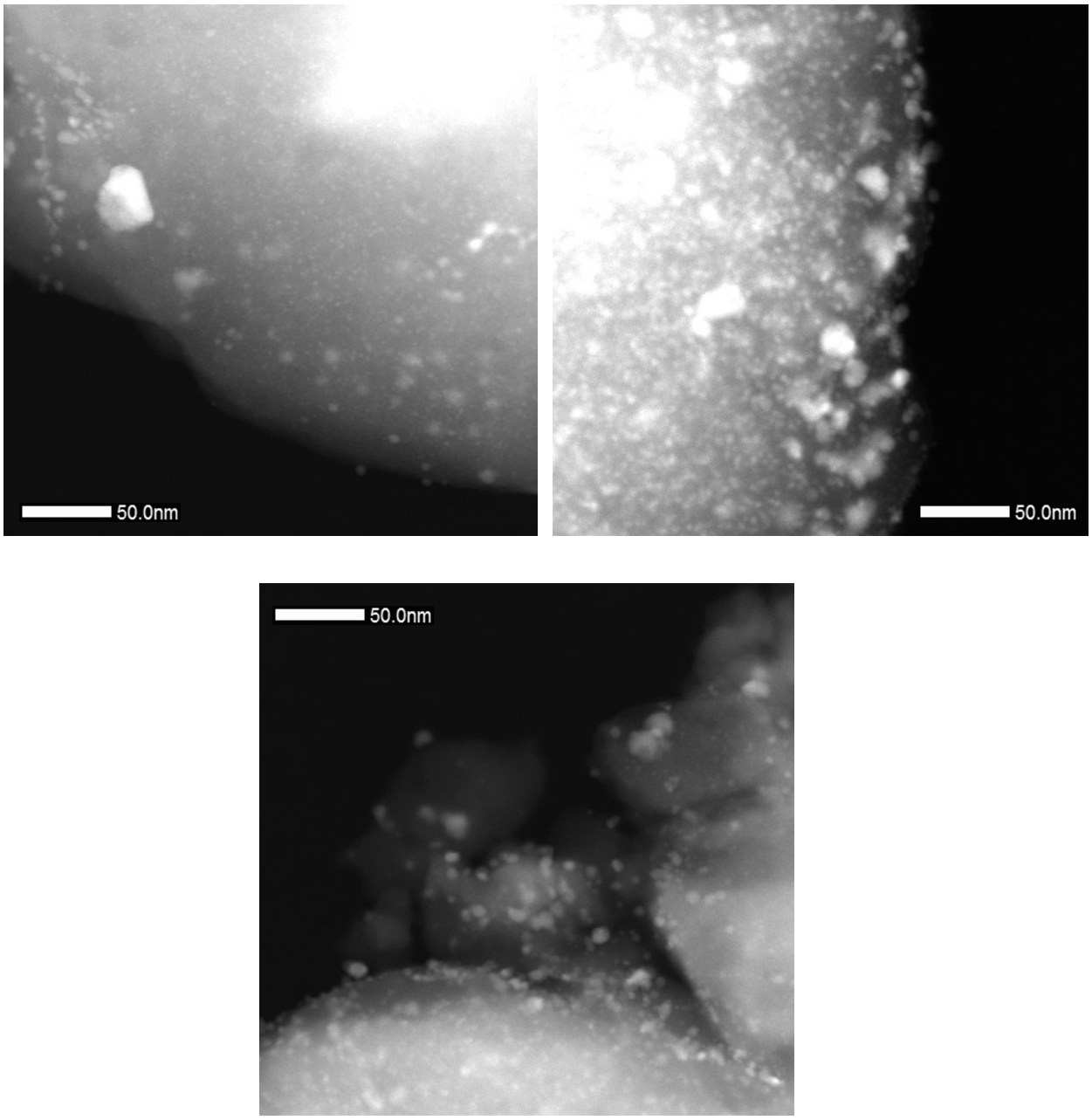

Figure S15. Representative HAADF-STEM images of Pd(2)/SSZ-13 (35) 750C 350V.